

# Gate Voltage Controlled Humidity Sensing Using MOSFET of VO<sub>2</sub> Particles

A. A. Akande, B. P. Dhonge, B. W. Mwakikunga, A. G. J. Machatine

**Abstract**—This article presents gate-voltage controlled humidity sensing performance of vanadium dioxide nanoparticles prepared from NH<sub>4</sub>VO<sub>3</sub> precursor using microwave irradiation technique. The X-ray diffraction, transmission electron diffraction, and Raman analyses reveal the formation of VO<sub>2</sub> (B) with V<sub>2</sub>O<sub>5</sub> and an amorphous phase. The BET surface area is found to be 67.67 m<sup>2</sup>/g. The humidity sensing measurements using the patented lateral-gate MOSFET configuration was carried out. The results show the optimum response at 5 V up to 8 V of gate voltages for 10 to 80% of relative humidity. The dose-response equation reveals the enhanced resilience of the gated VO<sub>2</sub> sensor which may saturate above 272% humidity. The response and recovery times are remarkably much faster (about 60 s) than in non-gated VO<sub>2</sub> sensors which normally show response and recovery times of the order of 5 minutes (300 s).

**Keywords**—VO<sub>2</sub>, VO<sub>2</sub> (B), V<sub>2</sub>O<sub>5</sub>, MOSFET, gate voltage, humidity sensor.

## I. INTRODUCTION

THE well-known phases of Vanadium oxides VO<sub>2</sub>, V<sub>2</sub>O<sub>3</sub> and V<sub>2</sub>O<sub>5</sub> with V<sup>4+</sup>, V<sup>3+</sup>, V<sup>5+</sup> ionic state (valence state) respectively, among other homologues series or members of the groups V<sub>n</sub>O<sub>2n</sub>, V<sub>n</sub>O<sub>2n-1</sub>, V<sub>n</sub>O<sub>2n+1</sub>, etc. have a significant impact on current research in the optical and electronic field [1]-[3]. The most interesting one among them is VO<sub>2</sub> because of its semiconductor-to-insulator transition around 340 K which is usually accompanied by a change in properties such as resistivity, conductivity, optical transmittance and reflectance [2]. All these properties have been reported to be preceded by phonon and electron interactions with crystal structure as it changes from low-temperature monoclinic M<sub>1</sub> phase (with space group *P*<sub>2</sub><sub>1</sub>/*c*) to high-temperature rutile phase R (with space group *P*<sub>4</sub><sub>2</sub>/*mnm*) and electronic band dimerization [2], [3]. However, VO<sub>2</sub> phase has been discovered to have many other polymorphs apart from the distorted M<sub>1</sub> and most stable R phases mentioned above. These other members are the meta-stable VO<sub>2</sub> (B), VO<sub>2</sub> (A), VO<sub>2</sub> (A<sub>H</sub>) [4], [5] and M<sub>2</sub> the intermediate phase between M<sub>1</sub> and R phase. These phases have been generally useful in technologies such as thermal switch (thermochromic window), thermal/infrared sensors,

ultrafast switches, optical modulators (optical gating), solid oxide fuel cell electrodes, chemical and humidity sensors [6], [7]. For example, humidity sensing of vanadium particles seated on Al<sub>2</sub>O<sub>3</sub>-Pt interdigitated electrode configuration has been demonstrated in the previous study [1].

In this report, the effect of gate voltage to the humidity response of mixed amorphous-crystalline VO<sub>2</sub> (B) in MOSFET configuration will be presented.

## II. METHODOLOGY

### A. Material Preparation

Synthesis of VO<sub>2</sub> powders was achieved through microwave irradiation. The precursor NH<sub>4</sub>VO<sub>3</sub> (purity 99.99%) and oxalic reagent are thoroughly dissolved in deionized water. The solution was transferred into 100 mL Teflon vessel and placed onto Multiwave 3000 microwave reactor. The reactor power, temperature and the reaction time were maintained at 600 W, 180 °C and 20 minutes, respectively. The synthesised sample was allowed to cool for 30 minutes and washed repeatedly with organic solvents in an ultrasonic bath to remove impurity and to minimize agglomeration. Finally, the sample was dried at 100 °C for 12 h.

### B. Material Characterization

The characterization techniques used to analyse this material are: Panalytical X' pert Pro PW 3040/60 (XRD) with Cu K<sub>α</sub> (λ=0.154 nm) monochromatic radiation and Jobin-Yvon T64000 Raman spectrograph (RS) with argon ion laser (power 0.384 mW) operated in 514.5 nm excitation wavelength for structural analyses and JEOL 2100 transmission electron microscopy (TEM) for the morphological studies.

### C. Phisorption Test, VO<sub>2</sub> MOSFET Fabrication and Humisity Sensing Measurements

Adsorption and desorption isotherm to N<sub>2</sub> molecule was carried out using Brunauer-Emmett-Teller (BET) Micromeritics TriStar II series Surface Area, Porosity instrument and degassing system from the USA.

The VO<sub>2</sub> MOSFET was fabricated by ultrasonically dispersing the VO<sub>2</sub> particles in the organic solvent for 30 minutes and drop-casted onto drain-gate-source electrodes. The connection configuration MOSFET is developed in our group [8].

Humidity sensing measurements were conducted using KSGA565 KENOSISTEC instrument from Italy. VO<sub>2</sub> MOSFET was situated in the chamber and connected to the KEITHLEY source-metre incorporated in the system. The instrument set-up and sample preparation details are reported

A.A Akande holds PhD studentship candidate position at DST/CSIR National Centre for Nano-Structured Materials but registered as a PhD student at the University of Pretoria (e-mail: aaakande@csir.co.za).

B. W. Mwakikunga is a Principal Research Scientist at the DST/CSIR National Centre for Nano-Structured Materials (e-mail: bmwakikunga@csir.co.za).

B. P Dhonge is a Post-Doctoral Scientist at DST/CSIR National Centre for Nano-Structured Materials

A.G.J Machatine is a Senior Lecturer at the School of Physics University of Pretoria

elsewhere [9]. Humidity measurements were performed for relative humidity ranging from 15 to 80% at different gate voltages.

### III. RESULTS AND DISCUSSION

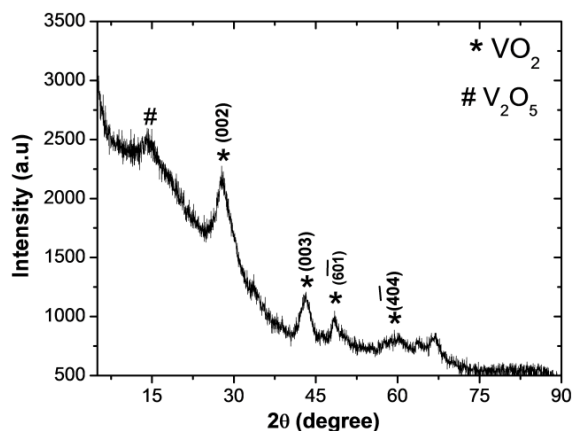


Fig. 1 XRD pattern of VO<sub>2</sub> particles

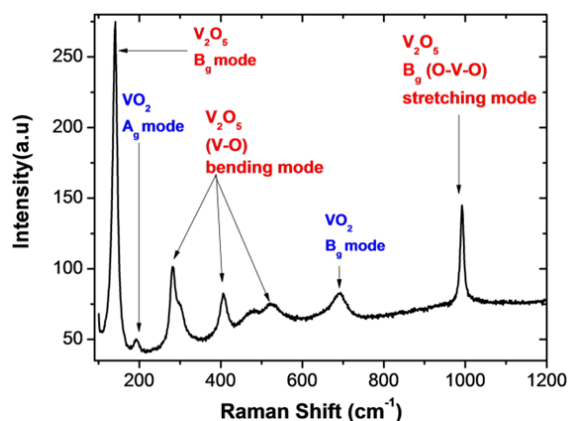


Fig. 2 Raman spectrum of VO<sub>2</sub> particles

The crystal structure of the VO<sub>2</sub> particles is shown by the XRD spectrum in Fig. 1. The spectrum clearly shows that the phase produced herein is VO<sub>2</sub> (B) with trace presence of V<sub>2</sub>O<sub>5</sub> and amorphous phase of both V<sub>2</sub>O<sub>5</sub> and VO<sub>2</sub> (B). The low angle peak at 15° (2θ) is the characteristic peak of V<sub>2</sub>O<sub>5</sub> (PCDPDFWIN CAS No: 89-0611). This evidence shows that the precursor NH<sub>4</sub>VO<sub>3</sub> has undergone reduction process in the following order: NH<sub>4</sub>VO<sub>3</sub> → V<sub>2</sub>O<sub>5</sub> → VO<sub>2</sub>. This order of formation is validated by the fact that NH<sub>4</sub>VO<sub>3</sub> has the vanadium ion in the V<sup>5+</sup> state similar to that of V<sub>2</sub>O<sub>5</sub>. Reduction from V<sup>5+</sup> of V<sub>2</sub>O<sub>5</sub> to V<sup>4+</sup> in VO<sub>2</sub> requires extra energy which is provided from calcination. Moreover, the phase VO<sub>2</sub> (B) has been widely reported in the literature as the preferred phase microwave synthesis and other hydrothermal techniques [4], [5]. Many phases VO<sub>2</sub> (B) were identified and index, the broad and intense peak at angle 27.8 (2θ) with (002) reflection, the peak at 43.5 (2θ) with (003) reflection and others according to the JCPDS 81 - 2392. The Raman spectrum, as shown in Fig. 2, reveals the peaks corresponding to VO<sub>2</sub> and

V<sub>2</sub>O<sub>5</sub> vibrational modes. The peaks belonging to V<sub>2</sub>O<sub>5</sub> phase seems to dominate in the spectrum because it is a very stable compared to the VO<sub>2</sub> phase of vanadium oxides. This means that the V<sub>2</sub>O<sub>5</sub> might be formed at the surface of the core crystalline VO<sub>2</sub>, hence Raman spectroscopy which is surface analysis technique captured more surface phonons than the core. A similar effect has been reported by Mwakikunga et al. [10] and Akande et al. [11].

The TEM image of the VO<sub>2</sub> particle in Fig. 3 (a) shows that the particles are composed of mixed crystalline grains and the amorphous phase. The first ring, in Fig. 3 (b), which presents the selected area electron diffraction (SAED) pattern, after the central undiffracted diffuse electron beam can be index to (002) Miller plane of the VO<sub>2</sub> (B) crystal structure. The second ring could be attributed to the second intense peak in XRD which also belongs to VO<sub>2</sub> (B). The TEM SAED agrees with XRD that VO<sub>2</sub> (B) is the dominant phase.

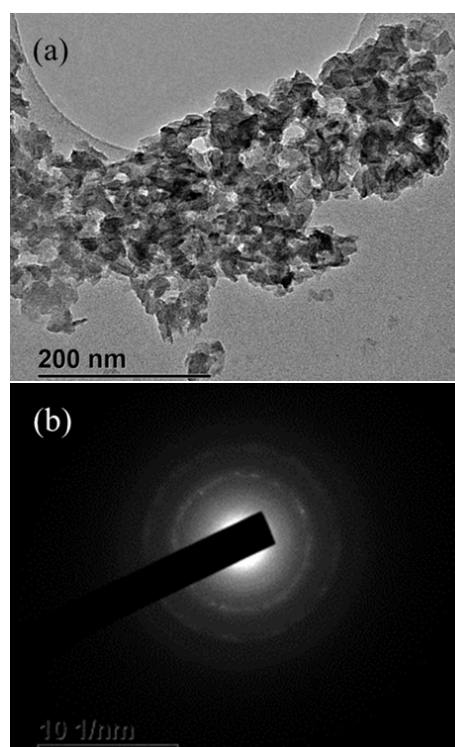


Fig. 3 (a) TEM of VO<sub>2</sub> particles, (b) selected area electron diffraction (SAED)

The BET surface area and physisorption adsorption/desorption isotherm shown in Fig. 4 show high detection capability of the VO<sub>2</sub> particles to N<sub>2</sub> molecules. The quantities in the figure showed improved physisorption effect compared with the one observed in the CVD synthesis of VO<sub>2</sub> [1]. The present surface area is found to be 67.67 m<sup>2</sup>/g compared to the maximum surface area value of about 16 m<sup>2</sup>/g in the previous finding.

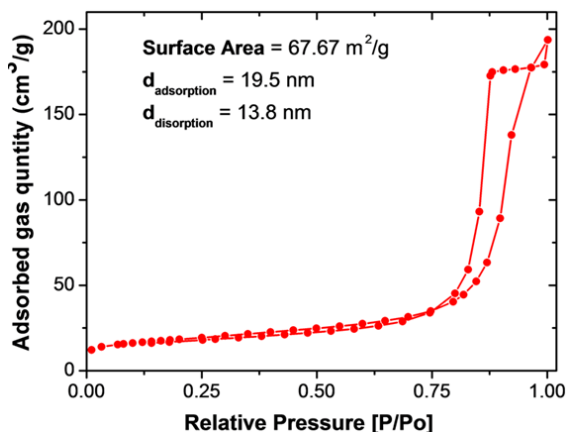


Fig. 4 N<sub>2</sub> molecule adsorption and desorption isotherms profile of VO<sub>2</sub> surface

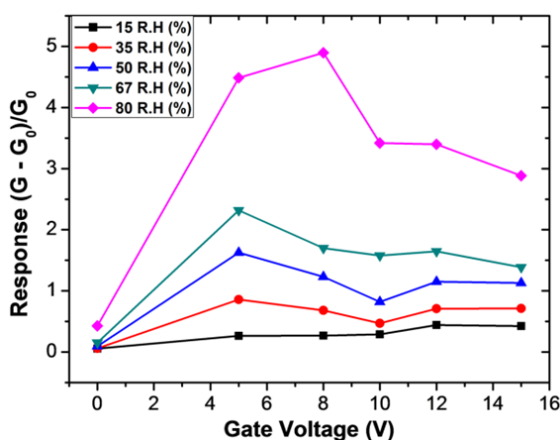


Fig. 5 Response of the VO<sub>2</sub> sensor to relative humidity versus the respective gate voltages

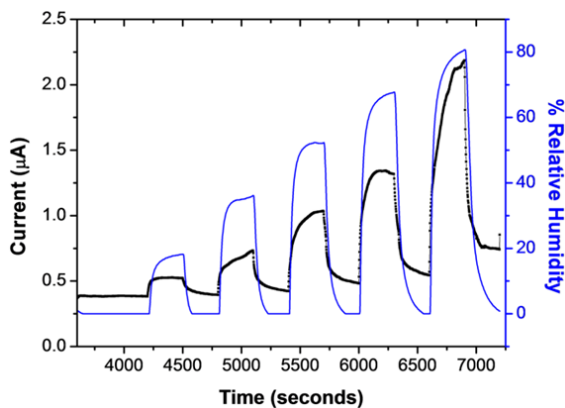


Fig. 6 Current-time curves for the sensor response to varying relative humidity concentrations. for gate of 5 V

The humidity sensing measurement was carried out at  $-V$  of the drain to source voltage. The gate voltages ( $V_g$ ) was varied from 0 to 15 V. The sensing device response to various humidity level for different gate voltages is shown in Fig. 5. The optimum gate voltage was found to be 5 V. The reason for

the 5-V optimum response can be attributed to an effect similar to response-temperature curves in traditional thermally-activated sensors. In such thermally-activated sensors, there exists an optimum temperature at which one gets the maximum response. At lower than this critical temperature, it is known that one gets adsorption increasing with temperature. At higher than this critical temperature, the semiconductor properties, where resistance decreases with rising temperature, dominate the adsorption effect. The analogy here is that the heater under the traditional sensor is replaced with a gate or bias voltage. At lower than the critical gate voltage, the adsorption of water vapor molecule effect dominates any other mechanisms available. At higher than this voltage the transistor is driven its pinch-off state where reduced current leads to drastic reduction in response to the adsorbing water vapor molecules. The pinch-off state is synonymous to either the Gunn Effect or the Josephson's junction effect where negative resistance has been reported for this configuration of transistors in the patent [8].

The change with respect to time in the source to drain current with various percentages of humidity at  $V_g = 5$  V is shown in Fig. 6. The response time is typically 60 s and recovery time is 70 s. This is very quick response and recovery when compared to the previous VO<sub>2</sub>(B) sensor.

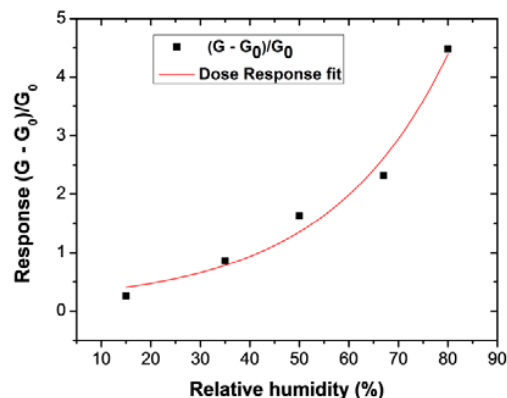


Fig. 7 Non-linear profile of the response to humidity as a function of the level of the relative humidity

When one considers the response to humidity as a function of the level of the relative humidity as shown in Fig. 7, one observes a non-linear profile which is symptomatic of S-shaped curves in dose-response characteristic equation such as that of Hill, Boltzman S – equation or the dose-response equation. When the three equation were tried for fitting, the does-response equation given by

$$G_{res} = \frac{G - G_0}{G_0} = A_1 + \frac{A_2 - A_1}{1 + 10^{(\log RH_0 - RH)p}} \quad (1)$$

where  $A_1$  and  $A_2$  are the lowest and highest sensor responses  $\log(RH_0)$  is the logarithm of the relative humidity at 50% response whereas EC50 is the antilogarithm of  $\log(RH_0)$  dose at which 50% response is achieved by the sensor and  $p$  is the Hill factor. From the fitting, EC50 value is 272%,  $p = 1.26 \times$

10272 whereas  $\log(RH_0)$  is 272.1, A1 and A2 are respectively 0.118 and 12096 with a correlation coefficient,  $R^2$ , of 0.925. These results suggest that the  $VO_2$  sensor is very resilient to humidity such that it does not saturate even when humidity approaches 100%. This sensor can then withstand rainy conditions.

#### IV. CONCLUSION, ON-GOING STUDIES

The nanostructured vanadium oxide was successfully synthesised and used for the humidity sensing measurements in MOSFET configuration. The gate voltage was optimized to  $V_g = 5$  V. The high intensity peak of  $V_2O_5$  vibration modes observed in Raman spectra reveals the formation of core-shell structure. The presence of  $V_2O_5$  phase with amorphous background was also observed in XRD and TEM measurements. The BET surface area was found to be  $67.67 \text{ m}^2/\text{g}$ . The response and recovery times of the gated sensor are remarkably greater (of the order of 60-70 s) than the non-gated  $VO_2$  sensor (which showed time of more than 300 s). The response-humidity data are non-linear and follow the typical S-curve profile. The response-dose equation fits the response-humidity data better than the Hill or Boltzmann S-curve equations and it is found that the sensor is very resilient to humidity by showing a humidity level of more than 100% where the response of the sensor could be reduced to 50%.

#### ACKNOWLEDGMENT

Authors acknowledge the support from the CSIR Advanced Materials for Device Applications programme (HGER27S) and the two programmes viz: India-Brazil-South Africa trilateral cooperation (HGER24X) and SA-Taiwan bilateral (HGER31X) under the National Research Foundation (NRF) grant number.

#### REFERENCES

- [1] A.A. Akande, E.C. Liganiso, B.P. Dhonge, K.E. Rammutla, A. Machatine, L. Prinsloo, H. Kunert, B.W. Mwakikunga, "Phase evolution of vanadium oxides obtained through temperature programmed calcinations of ammonium vanadate in hydrogen atmosphere and their humidity sensing" *J of Mat. Chem. and Phy.* 151, 206, April 2015.
- [2] A.A. Akande, K. E. Rammutla, T. Moyo, N. S.E. Osman, Steven S. Nkosi, C.J. Jafta, and Bonex W. Mwakikunga, "Magnetism variations and susceptibility hysteresis at metal-insulator phase transition of  $VO_2$  in a composite film containing vanadium and tungsten oxides" *J Magn. Magn. Mater.* 375, Feb. 2015.
- [3] E. Volker "The metal-to-insulator transitions of  $VO_2$ : A band theoretical approach" *Ann. Phy Leipzig* 11 (1-6) (2002) 9
- [4] E. Strelcov, Y. Lilach, A. Kolmakov, "Gas sensor based on metal to insulator transition in  $VO_2$  nanowire thermistor" *Nano Lett.* 9 (2009) 2322-2322
- [5] C. Wang, X. Liu, W. Xiong, Y. Zheng, "PEG-Assisted hydrothermal synthesis of  $VO_2$  (A) nanowire with remarkable optical switching properties" International Conference on Mechanics and structural Engineering (ICMSE 2016)
- [6] Z. Yang, C. Ko, S. Ramanathan, "Oxide Electronics Utilizing Ultrafast Metal to Insulator Transitions" *Annu. Rev. Mater. Res.* 41 (2001) 337-367
- [7] M. Maaza, O. Nemraoui, C. Sella, A. C. Beye and B. Baruch-Barak, Thermal induced tunability of surface plasmon resonance in Au- $VO_2$  nano-photonics, *Optics Comm.* 254 (2005) 188-195.
- [8] B. W. Mwakikunga, A field effect transistor and a gas detector including a plurality of field effect transistors, PA158013/P No. WO2014191892
- A1 PCT/IB2014/061713 also published as China (CN105474006A) Germany (DE112014002575T5) and USA (US20160116434)
- [9] A.A. Akande, B.W. Mwakikunga, K.E. Rammutla, A. Machatine, L., "Larger selectivity of the  $V_2O_5$  nano-particles sensitivity to  $NO_2$  than  $NH_3$ ," *J of Sensor and Transducers* 151, 206, Sept. 2015)
- [10] B. Mwakikunga, M. Maaza, K.t. Hillie, C.J. Arendse, T. Malwela, E. Sideras Haddad "From Phonon confinement to phonon splittings in flat single nanostructures, A case of  $VO_2@V_2O_5$  core-shell nano-ribbons," *Raman spectr.* (2012).
- [11] A.A. Akande "Vanadium dioxide Nanostructure Production and Applications in Sensors" MSc Thesis 2014 (Unpublished).